

[Preferential dissolution of U-rich zircon can bias the Hf isotope compositions of granites]

[Peng Gao^{1*}, Chris Yakymchuk², Jian Zhang¹, Changqing Yin¹, Jiahui Qian¹, Yanguang Li^{3*}]

[1. School of Earth Science and Geological Engineering, Sun Yat-sen University, Guangzhou 510275, China

2. Department of Earth and Environmental Sciences, University of Waterloo, Waterloo, Ontario, Canada, N2L 3G1

3. Xi'an Center of Geological Survey, China Geological Survey, Xi'an 710054, China]

* Corresponding author. E-mail: gaop8@mail.sysu.edu.cn (P. Gao); liyanguangok@126.com (Y. Li)

Contents of this file

Part I: Methodology

Part II: Figures DR1 to DR3

Part III: Calculations of garnet–zircon hafnium isotope model

Introduction

[This Data Repository provides the Methodology, and the additional Figures used in the present study (Figures DR1 to DR3)]

Part I: Methodology

1. LA(SS)-MC-ICPMS zircon analyses

Zircon grains were extracted, mounted and polished to expose grain centers for microbeam analyses. Cathodoluminescence (CL) images are taken for inspecting internal structures of individual zircons and selecting positions for U–Pb and Lu–Hf isotope and trace element in-situ analyses.

In situ zircon U–Pb dating and trace element analyses and Lu–Hf isotope analyses were performed using a Geolas Pro laser-ablation (LA) system simultaneously coupled to a Neptune Plus multiple-collector (MC) ICP-MS and a 7700x quadrupole ICP-MS at the Key Laboratory for the study of focused Magmatism and Giant ore Deposits of Ministry of Natural Resources, in Xi'an Center of Geological Survey, China Geological Survey. A stationary laser ablation spot with a beam diameter of 44 μm was used for the analyses. The ablated aerosol was carried by helium and then combined with argon via a T-connector before being introduced to the ICP-MS plasma. After smoothed, the sample gas will be split into two lines, one goes into quadrupole ICP-MS for zircon U–Pb dating and trace element analyses, the other goes into multiple-collector ICP-MS for Hf isotope analyses after combined with a bit of N_2 (4 ml/min) for sensitivity improvement.

During this study, zircon 91500 was used as primary (calibration) reference material for the U–Th–Pb isotope analyses. GJ-1 was used as the monitor

standard. Synthetic silicate glass NIST-610 was used to calibrate the trace element concentration data. Si was used as internal standard to correct for differences in the ablation yields between zircon and glass standards. Trace element concentrations and U–Pb isotopic ratios and ages were reduced and calculated using Lolite 4 ([Paton et al., 2011](#)), and Hf isotope was calculated using a in house software Hflow 3.4. Details of the instrumental conditions and data acquisition procedures are similar to those described by [Yuan et al. \(2008\)](#).

Fifty-four analyses of GJ-1 yielded a weighted mean $^{206}\text{Pb}/^{238}\text{U}$ age of 604.0 ± 3.2 Ma (2σ , MSWD = 1.03), which is in agreement with reference values obtained through ID-TIMS measurements reported in [Jackson et al. \(2004\)](#). Lu–Hf isotope data quality was monitored by the frequent analysis of reference zircons GJ-1, 91500, Plešovice and MUN-3 (a synthetic zircon doped with hafnium and rare earth elements). These reference zircons have a very wide range of $^{176}\text{Yb}/^{177}\text{Hf}$ ratios (0.005–0.22) and thus provides the best indication of the veracity of ^{176}Yb and ^{176}Lu interference corrections on ^{176}Hf . These $^{176}\text{Yb}/^{177}\text{Hf}$ values covered those measured from 100% of the zircons in our dataset. Values of $^{176}\text{Lu}/^{175}\text{Lu} = 0.02658$ and $^{176}\text{Yb}/^{173}\text{Yb} = 0.796218$ were used to correct for ^{176}Lu and ^{176}Yb isobaric interferences, respectively ([Chu et al., 2002](#)). Instrumental mass bias was accounted for by normalizing Yb isotope ratios to $^{172}\text{Yb}/^{173}\text{Yb} = 1.35274$ ([Chu et al., 2002](#)) and Hf isotope ratios to $^{179}\text{Hf}/^{177}\text{Hf} = 0.7325$ ([Patchett and Tatsumoto, 1980](#)), using an exponential mass fractionation law. The mass bias behavior of Lu was assumed to follow that of

Yb. For details on the mass bias correction protocols, see [Fisher et al. \(2011\)](#). Only a subset of dated GJ-1 have been analyzed for Lu–Hf isotope. The determined mean $^{176}\text{Hf}/^{177}\text{Hf}$ ratios of GJ-1, 91500, Plešovice and MUN-3 was 0.282008 ± 0.000009 ($n = 38$, 2SD), 0.282296 ± 0.000024 ($n = 18$, 2SD), 0.282488 ± 0.00009 ($n=6$, 2SD) and 0.282134 ± 0.000018 ($n = 19$, 2SD) respectively, which is in agreement within errors with reference values recommended by [Morel et al. \(2008\)](#), [Wiedenbeck et al. \(1995\)](#), [Slama et al. \(2008\)](#) and [Fisher et al. \(2011\)](#).

The isotopic ratios and ages reported for U–Pb isotope with 2σ propagated uncertainties are calculated by *iolite* and are uncorrected for common Pb. Only analyses with $<\pm 10\%$ discordance between their $^{206}\text{Pb}/^{238}\text{U}$ and $^{207}\text{Pb}/^{235}\text{U}$ ages are considered in our interpretations. The metadata for zircon U–Pb and Lu–Hf isotopic analyses of this study are provided in [Table DR1](#) following the recommended format of [Horstwood et al. \(2016\)](#); U–Pb isotopic compositions of zircon standards used in this study are listed in [Table DR2](#); Lu–Hf isotopic compositions of the zircon standards used in this study are listed in [Table DR3](#); zircon trace element and U–Pb and Lu–Hf isotope data for samples are listed in [Table DR4](#).

2. Whole-rock major-trace element analyses

Whole-rock major and trace elements were analyzed at the ALS Chemex (Guangzhou, China) Co., Ltd. Major element oxides were determined using an X-ray fluorescence spectrometer (XRF). Analytical precision of major element

oxides is better than ± 2 -5%. Trace elements were determined using PerkinElmer ICP-MS with the analytical precision better than $\pm 5\%$ for most elements. Whole-rock major-trace element analyses are listed in [Table DR5](#).

3. Detrital zircon data compiled from literature

Ages, Th and U concentrations, and Hf isotopic compositions for detrital zircon of the Himalayan sedimentary strata were compiled from [Spencer et al. \(2012\)](#) and [Wang et al. \(2016\)](#), and are provided in [Table DR6](#).

4. Modelling of garnet and zircon Hf isotope ratios

To evaluate the potential role of a high Lu/Hf minerals in the source and their impact on melt extracted from the source (from which autocrystic zircon crystallized), we conducted a simplified mass balance model. At 20 Ma, zircon is assumed to have a $^{176}\text{Hf}/^{177}\text{Hf}$ ratio of 0.282412 and a $^{176}\text{Lu}/^{177}\text{Hf}$ ratio of 0.00143; these are medians of the values in this study for inherited zircon ([Table DR4](#)). This zircon is assumed to have a Hf concentration of 12,000 ppm (average of this study; [Table DR4](#)) and make up 0.01 wt% of the model source rock (equivalent to 50 ppm Zr in bulk, lower bound for metapelite; c.f. [Yakymchuk and Brown, 2014](#)). Garnet is assumed to make up 10 wt% of the source (approximate abundance for Himalayan metapelite, the potential source of Himalayan granite, according to [Patiño Douce and Harris, 1998](#) and [Bartoli, 2021](#)) and has an assumed concentration of 0.1 ppm Hf, which is an average of the values for Greater Himalayan garnet reported in [Anczkiewicz et al. \(2014\)](#).

Four scenarios are modelled for radiogenic ingrowth of Hf in garnet, which

represent the known range of $^{176}\text{Lu}/^{177}\text{Hf}$ values in garnet from the greater Himalaya ([Anczkiewicz et al., 2014](#)) using model $^{176}\text{Lu}/^{177}\text{Hf}$ ratios of 5, 10, 20 and 30. At 20 Ma, we model the $^{176}\text{Hf}/^{177}\text{Hf}$ composition of garnet assuming that various amounts of time have passed since garnet growth (i.e. garnet residence time); these vary from 0 Myr before 20 Ma—a approximation for garnet growth at the same time as melt extraction—up to 30 Myr before 20 Ma, which is an extreme scenario where garnet resided in the crust for 30 Myr before melt was extracted at 20 Ma to form the granites in this study, i.e. garnet with ages of 50 Ma that have been reported from the Tibetan plateau ([Smit et al., 2014](#)). We assume that the starting composition of the source from which the garnet grew has a $^{176}\text{Hf}/^{177}\text{Hf}$ ratio of 0.282412, which is the same as the inherited zircon at 20 Ma.

This modelling assumes that all garnet dissolves during partial melting, which is unrealistic as garnet is a peritectic mineral during partial melting, i.e. it is stable and growing during partial melting ([Yakymchuk and Brown, 2014](#)). Furthermore, the duration of garnet residence assumes garnet resides in the crust and accumulates radiogenic ^{176}Hf for millions of years. Partial melting, garnet growth and melt extraction are generally not expected to take tens of millions of years in the Himalayan system (c.f. [Ayres et al., 1997](#)). Therefore, our modelling represents an extreme scenario for radiogenic ingrowth of ^{176}Hf in metasedimentary migmatites in the Himalaya.

Part II: Figures

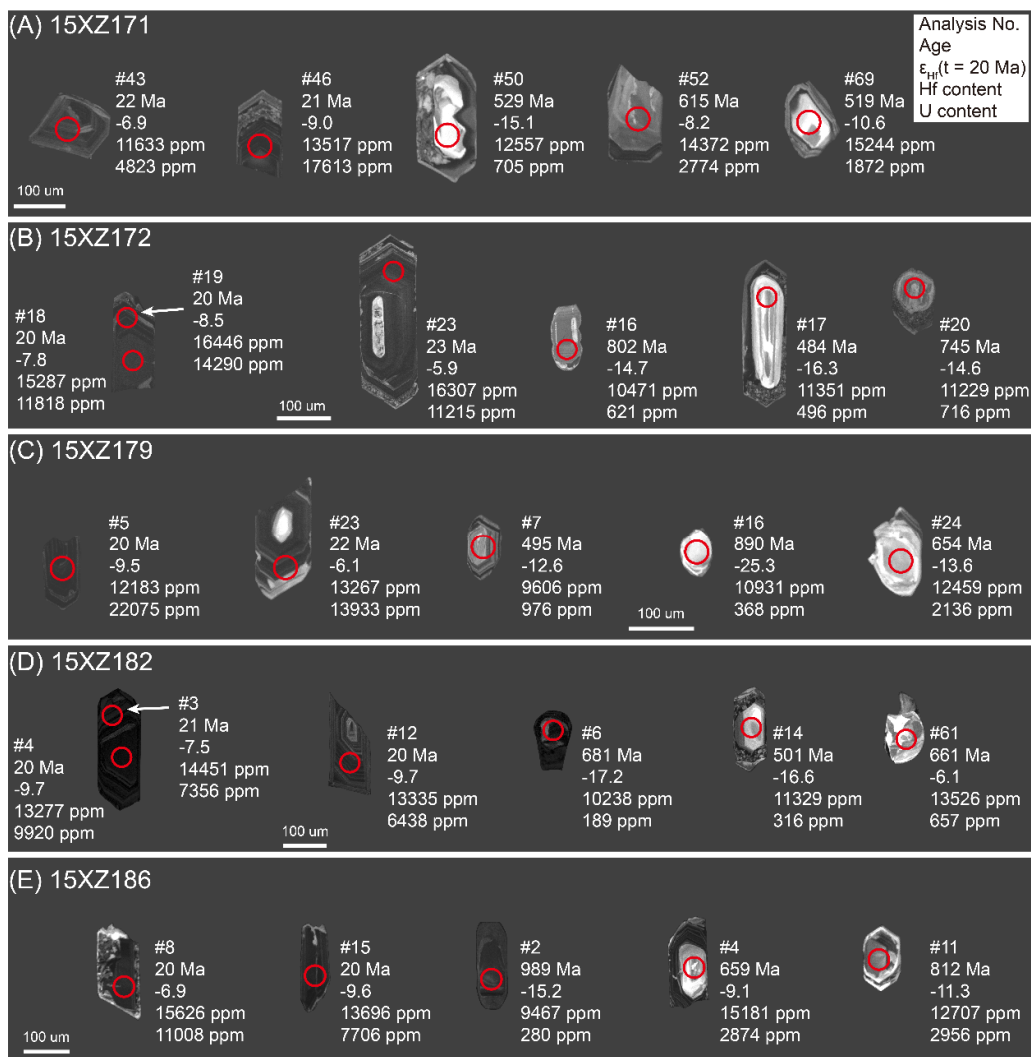


Figure DR1. CL images of representative zircons from the Nariyongcuo granites. The red circles are analytical positions, with diameters of 44 μm . Analytical No., analytical results of U–Pb ages, $\epsilon_{\text{Hf}}(t)$ values and Hf and U contents are also labeled.

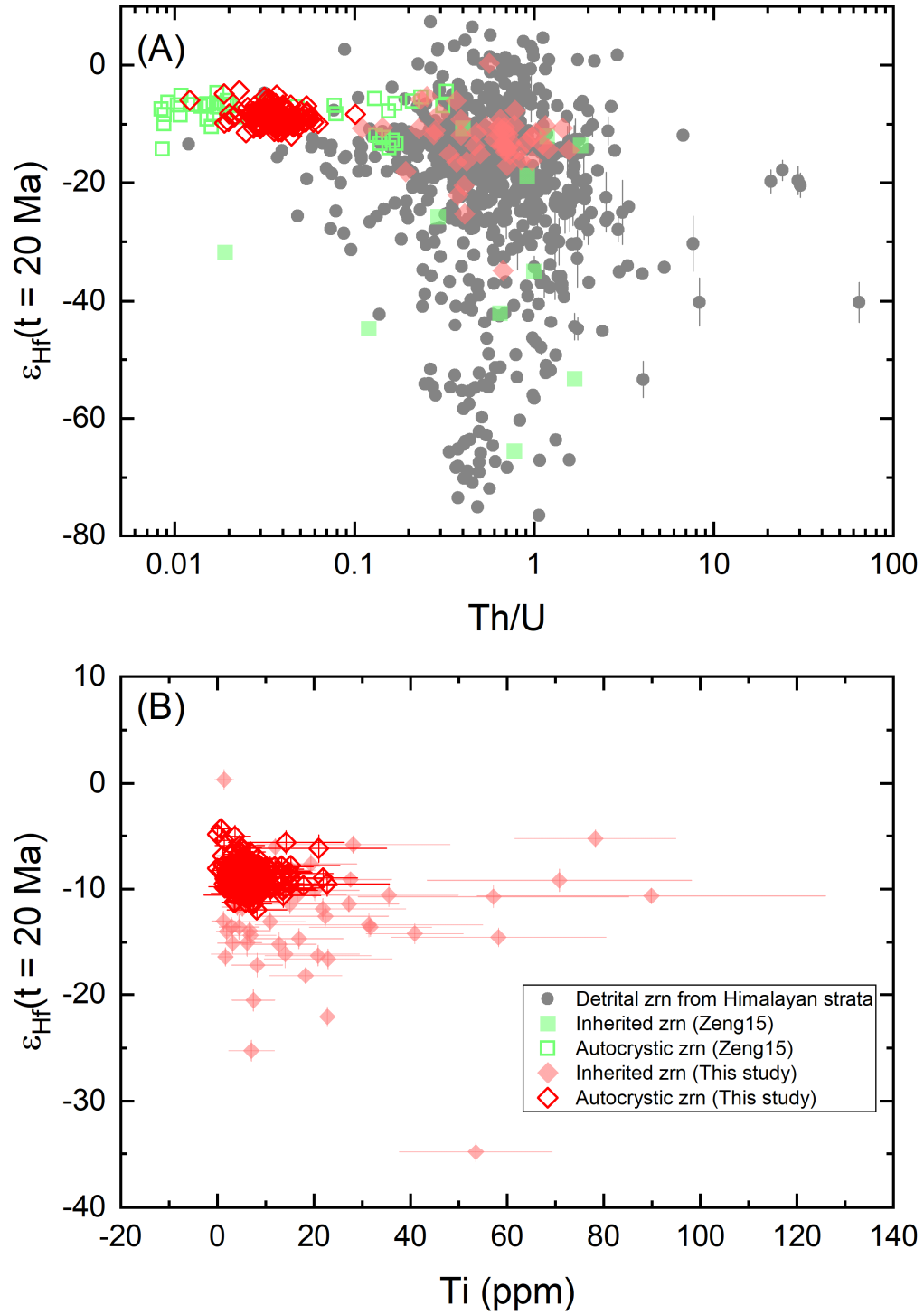


Figure DR2. (A) Plot of zircon (zrn) Th/U ratios versus $\epsilon_{\text{Hf}}(t)$ values for the Nariyongcuo granites, compared with zircon from other Himalayan granites (Zeng et al., 2015) and detrital zircon from Himalayan strata (Spencer et al., 2012; Wang et al., 2016). Errors are in 2σ and smaller than the symbol when not shown. (B) Plot of Ti concentrations versus $\epsilon_{\text{Hf}}(t)$ values of zircon for the Nariyongcuo granites. Errors are in 2σ .

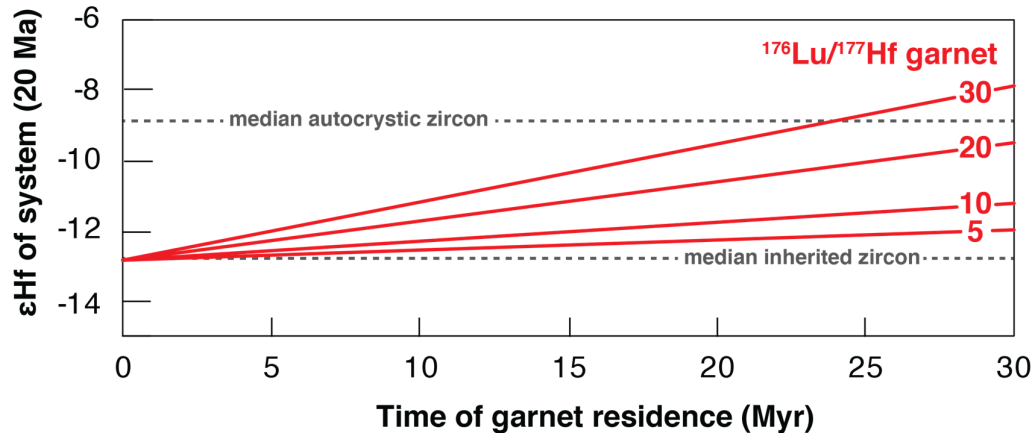


Figure DR3. Mass balance modeling results showing the influence of garnet dissolution on the isotopic composition of the system for four scenarios where garnet has different $^{176}\text{Lu}/^{177}\text{Hf}$ ratios (i.e. different amounts of radiogenic ^{176}Hf ingrowth). Also plotted are the median values of autocrystic and inherited zircon (at 20 Ma) from Table DR4. For the median value of inherited zircon to reach the median autocrystic zircon, an extreme $^{176}\text{Lu}/^{177}\text{Hf}$ ratio of garnet >20 is needed, as well as >20 Myr of residence time in the crust prior to complete garnet dissolution.

References

- Anczkiewicz, R., Chakraborty, S., Dasgupta, S., Mukhopadhyay, D., and Kořtonik, K., 2014, Timing, duration and inversion of prograde Barrovian metamorphism constrained by high resolution Lu–Hf garnet dating: A case study from the Sikkim Himalaya, NE India: *Earth and Planetary Science Letters*, v. 407, p. 70–81.
- Ayres, M., Harris, N. and Vance, D., 1997. Possible constraints on anatectic melt residence times from accessory mineral dissolution rates: an example from Himalayan leucogranites: *Mineralogical Magazine*, v. 61, p.29-36.
- Bartoli, O., 2021, Granite geochemistry is not diagnostic of the role of water in the source: *Earth and Planetary Science Letters*, v. 564, p. 116927.
- Chu, N.C., Taylor, R.N., Chavagnac, V., Nesbitt, R.W., Boella, R.M., Milton, J.A., German, C.R., Bayon, G., Burton, K., 2002. Hf isotope ratio analysis using multicollector inductively coupled plasma mass spectrometry: an evaluation of isobaric interference corrections. *J. Anal. At. Spectrom.* 17, 1567–1574.
- Elhlou, S., Belousova, E., Griffin, W.L., Pearson, N.J., O’Reilly, S.Y., 2006. Trace element and isotopic composition of GJ–Red zircon standard by laser ablation. *Geochim. Cosmochim. Acta*, 70, 158.

- Fisher, C.M., Hanchar, J.M., Samson, S.D., Dhuime, B., Blichert-Toft, B., Vervoort, J.D., Lam, R., 2011. Synthetic zircon doped with hafnium and rare earth elements: A reference material for in situ hafnium isotope analysis. *Chemical Geology*, 286, 32–47.
- Horstwood, M.S.A., Košler, J., Gehrels, G., Jackson, S.E., McLean, N.M., Paton, C., Pearson, N.J., Sircombe, K., Sylvester, P., Vermeesch, P., 2016. Community - derived standards for LA - ICP - MS U - (Th -) Pb geochronology - Uncertainty propagation, age interpretation and data reporting. *Geostandards and Geoanalytical Research*, 40, 311-332.
- Jackson, S.E., Pearson, N.J., Griffin, W.L., Belousova, E.A., 2004. The application of laser ablation-inductively coupled plasma-mass spectrometry to in situ U–Pb zircon geochronology. *Chemical Geology*, 211, 47–69.
- Morel, M.L.A., Nebel, O., Nebel-Jacobsen, Y.J., Miller, J.S., Vroon, P.Z., 2008. Hafnium isotope characterization of the GJ-1 zircon reference material by solution and laser-ablation MC-ICPMS. *Chemical Geology*, 255, 231-235.
- Patchett, P.J., Tatsumoto, M., 1980. Lu–Hf total-rock isochron for the eucrite meteorites. *Nature*, 288, 571–574.
- Patiño Douce, A.E., and Harris, N., 1998, Experimental constraints on Himalayan anatexis: *Journal of Petrology*, v. 39, p. 689–710.
- Paton, C., Hellstrom, J., Paul, B., Woodhead, J., Hergt, J., 2011. Lolite: Freeware for the visualisation and processing of mass spectrometric data. *Journal of Analytical Atomic Spectrometry*, 26, 2508-2518.
- Slama, J., Kosler, J., Condon, D.J., Crowley, J.L., Gerdes, A., Hanchar, J.M., Horstwood, M.S.A., Morris, G.A., Nasdala, L., Norberg, N., Schaltegger, U., Schoene, B., Tubrett, M.N., Whitehouse, M.J., 2008. Plesovice zircon-a new natural reference material for U–Pb and Hf isotopic microanalysis. *Chemical Geology*, 249, 1–35.
- Smit, M.A., Hacker, B.R., and Lee, J., 2014, Tibetan garnet records early Eocene initiation of thickening in the Himalaya: *Geology*, v. 42, p. 591–594.
- Spencer, C.J., Harris, R.A., Dorais, M.J., 2012. Depositional provenance of the Himalayan metamorphic core of Garhwal region, India: Constrained by U–Pb and Hf isotopes in zircons. *Gondwana Research*, 22, 26–35.
- Spencer, C.J., Kirkland, C.L., Roberts, N.M.W., Evans, N.J., Liebmann, J., 2020. Strategies towards robust interpretations of in situ zircon Lu–Hf isotope analyses. *Geoscience Frontiers*, 11, 843-853.
- Wang, J.G., Wu, F.Y., Garzanti, E., Hu, X., Ji, W.Q., Liu, Z.C., Liu, X.C., 2016. Upper Triassic turbidites of the northern Tethyan Himalaya (Langjiexue Group): The terminal of a sediment-routing system sourced in the Gondwanide Orogen. *Gondwana Research*, 34, 84-98.
- Wiedenbeck, M., Alle, P., Corfu, F., Griffin, W.L., Meier, M., Oberli, F., Quadt, A.V., Roddick, J.C., Spiegel, W., 1995. Three natural zircon standards for U–Th–Pb, Lu–Hf, trace element and REE analyses. *Geostand. Newsl.* 19, 1–23.
- Yakymchuk, C., and Brown, M., 2014, Behavior of zircon and monazite during crustal melting: *Journal of the Geological Society, London*, 171, 465-479.
- Yuan, H.L., Gao, S., Dai, M.N., Zong, C.L., Günther, D., Fontaine, G. H., X. M. Liu, Diwu,

C.R., 2008. Simultaneous determinations of U-Pb age, Hf isotopes and trace element compositions of zircon by excimer laser-ablation quadrupole and multiple-collector ICP-MS. *Chemical Geology*, 247, 100-118.